

# Mushy zones with fully developed chimneys

T. P. Schulze  
Department of Mathematics  
University of Tennessee  
Knoxville, TN 37996-1300

M. Grae Worster  
Institute of Theoretical Geophysics  
Department of Applied Mathematics and Theoretical Physics  
University of Cambridge, Silver Street, Cambridge CB3 9EW , UK.

December 5, 2000

## **Abstract**

Convection in mushy zones can lead to several types of free boundaries requiring distinct boundary conditions depending on whether the interface is freezing or melting and on the direction of flow relative to the interface. Here we implement these boundary conditions for the first time to arrive at solutions for mushy zones featuring liquid inclusions and fully developed chimneys.

# 1. Introduction

The modeling and analysis of convection within mushy zones has received much attention in the past two decades (Beckerman & Wang 1995, Worster 1999). A central object of study has been the formation of “chimneys” within the mushy layer. Chimneys occur when the convection of solute-depleted material redissolves dendrites as it flows from cooler to warmer regions within the mushy layer. The enhanced permeability of the dendrite-free region results in the formation of a focused plume. Interest in these features stems from both metallurgical and geophysical applications, chimneys being known as “brine channels” in the sea-ice literature.

This problem is highly nonlinear, placing severe restrictions on what can be accomplished by analytic means. In particular, the readily accessible linear and weakly-nonlinear regimes do not feature chimneys because the convection is not strong enough to dissolve the dendrites. Attempts to find limits where the convection is strong (large Rayleigh number) or the mush has a low solid fraction have met with limited success— while a number of authors have presented scaling analyses that outline boundary-layer structure, the resulting equations have not been solved and formally matched. In the paper by Amberg & Homsy(1993) a distinguished limit is taken in which the solid fraction has the same order of magnitude as the amplitude of convection. It is then possible to capture the first appearance of negative solid fraction within the weakly nonlinear theory. Because the mush–liquid interface was fixed, however, the solid fraction was negative first at the interface.

Numerical work faces its own challenges owing to the complicated nature of this free-boundary problem. Most numerical studies have been developed in the metallurgical community (Beckermann & Wang 1995) and aim to follow the time-evolution of castings without fully resolving mush–liquid boundaries, relying instead on interface-smearing and a Darcy-Brinkman model for momentum transport. While these studies may feature chimneys and are interested in macro-segregation, there has been no attempt to isolate a single, steady chimney and there have been few attempts to calibrate these numerical experiments against known theoretical results. An alternative approach has been to adopt models with explicit free boundaries favored in the analytic work. In this case, the focus is naturally placed on steady states that arise in a crystal-pulling context. To date, numerical work has only addressed the convective regime without chimneys (Schulze & Worster 1999) or resolved chimneys by introducing approximations that impose the shape of the free boundaries (Roberts & Loper 1983, Schulze & Worster 1998).

The present paper aims to extend this latter work to calculate steadily propagating solutions featuring liquid inclusions and fully developed chimneys. The following section for-

mulates the problem and includes a discussion of the choices we have made both in modeling the system and in seeking numerical solutions. A special effort has been made to contrast the two approaches identified above—a single-domain Darcy-Brinkman formulation versus a sharp-interface formulation. The third section describes more succinctly the methodology used in this work, with the final section reporting the results of these computations.

## 2. Discussion of Formulation and Solution Method

To fix ideas further, we begin by describing a sequence of steady flow configurations within a two-dimensional mushy zone which is being grown at a constant rate  $V$ . Figures 1-2 depict a mush-liquid system with either a liquid inclusion or a chimney and stream-lines corresponding to the material volume-flux vector

$$\mathbf{q} = -V\hat{\mathbf{k}} + \mathbf{U}(1 - \phi),$$

where  $\mathbf{U}$  is the mean interstitial fluid velocity relative to the solid phase and  $\phi$  is the solid fraction. Within the liquid region, these streamlines are particle paths. For weakly convecting solutions all of the streamlines would enter the top of the mushy zone and exit at the bottom, which we take to be a flat and uniformly propagating eutectic front. Such solutions (not shown here) are distinguished from the purely conductive state by the curvature of the streamlines, which indicates that the down-flow is being slowed by solutal buoyancy. For flow amplitudes that are somewhat stronger, the buoyancy will produce a steadily recirculating region fully contained within the mushy layer, but not strong enough to completely dissolve the dendrites. Figure 1 shows the result of a flow that is somewhat stronger still, so that a liquid inclusion has formed within the mushy zone. Finally, in Figure 2, we see a fully developed chimney with a buoyant plume emerging from the mushy zone.

The complicated nature of this free-boundary problem resists numerical treatment for a number of reasons: potential discontinuity of various quantities across the interface; boundary layers attached to the interface; changes in topology and changes in the boundary conditions themselves as one moves from one region of the interface to another (*e.g.* from a solidifying to a dissolving section). Given these difficulties, it is tempting to attack this problem with the Darcy-Brinkman formalism that has been popular in the casting-simulation literature. This approach seems to offer the promise of a single computational domain and *a posteriori* interface evaluation. A careful consideration of the physics, however, reveals that these advantages are less than they might at first appear and that they come with some reduced accuracy.

First, one must be able to identify which “phase” of matter a material point resides in—pure liquid or mushy zone—so that one either enforces a liquidus constraint or allows the concentration and temperature to evolve independently of one another. One way or another, this requires a check on a grid-point by grid-point basis so that one crudely tracks the interface location even in an otherwise single-domain approach. Further, the conditions which determine the precise location of this interface depend on whether the interface is solidifying or dissolving, and the equation which determines the solid fraction within the mushy zone is inherently hyperbolic. Thus, one must take care to sweep through the grid in a specific order. The appropriate order for doing this is evidently vertical moving away from a solidifying boundary when the problem is steady, but it is less clear what is appropriate for time-varying solutions. To do this correctly, one must know where the interface is. The single-domain approach also assumes continuity of various quantities (temperature, concentration, solid-fraction, velocity) as well as their derivatives. These assumptions introduce errors for at least two reasons. With respect to momentum transport, there is the issue of the no-slip condition and a question as to what length-scale the vorticity should relax between regions which are governed by momentum operators that are inherently second-order within the mushy region and fourth-order in the liquid region. With respect to the thermal boundary conditions, one has to question whether the solid fraction is indeed zero at the interface. If it is not, there are discontinuities in the concentration and thermal gradient. The second derivative of the thermal field will be discontinuous even with a zero-solid-fraction interface if the gradient of the solid fraction or the Stefan number is not also zero.

For these reasons, we believe caution is warranted and have aimed to perform careful studies focusing on a single convection cell with sharp interfaces. By adopting the crystal-pulling configuration, we are able to check the linear critical point for the onset of convection in our numerical experiments against analytic results. We are also able to verify the direction – sub- or super-critical – of the initial bifurcation. By focusing on steady solutions, we are able to eliminate complicated flows which might mask errors in our numerical methods. Finally, by neglecting solutal diffusion we eliminate boundary layers near the mush–liquid interface which are both difficult to resolve and a source of fine-scale convection, which itself presents even greater numerical difficulties. This latter assumption comes at the cost, however, of further complicating the free-boundary formulation.

Ideally, we would like to apply the boundary conditions given by Schulze and Worster (1999) to liquid-inclusion and chimney topologies. This paper comes close to that goal, but makes some concessions to simplify the numerical treatment of the problem. The complicated shapes of these domains make the boundary-mapping approach used by Schulze and Worster undesirable. Instead, we have adopted a fixed-grid approach with interpola-

tion, where necessary, to determine interfacial quantities. The additional assumptions are designed to minimize the need for interpolation, which is difficult on arbitrarily shaped interfaces. First, we assume that the Stefan number is zero so that no latent heat is produced at the interface. The result is that the heat equation is the same in both regions and, moreover, the temperature has a continuous derivative at the mush–liquid interface. Second we assume continuity of both velocity components at the interface rather than apply a no-slip or some other type of slip condition. As explained by Schulze and Worster, this condition is consistent with the no-slip condition along isotherms, which happen to coincide with large portions of the mush–liquid interface. Finally, we take the vorticity to be continuous across the mush–liquid interface in lieu of a continuous pressure.

This last assumption has no physical basis, but greatly simplifies the numerics by allowing one to use stream-function and vorticity data from one region to update those in the other. Our choice of this approach is dictated by our principal aim of demonstrating the thermal boundary conditions put forward by Schulze & Worster (1999). In particular, the condition

$$\mathbf{q} \cdot \nabla \theta = 0, \quad (2.1)$$

which should determine the location of solidifying interfaces with flow from mush to liquid, is acquitted here for the first time.

### 3. The equations

This section concisely presents the non-dimensionalized equations in the form in which they are actually solved in this paper; for further details of the formulation see the discussion above and consult Schulze & Worster (1998, 1999).

With the understanding that latent heat is being ignored, the heat equation is simply

$$\nabla^2 T + T_z = \mathbf{u} \cdot \nabla T,$$

where  $\mathbf{u} = (\mathbf{1} - \phi)\mathbf{U}$  is the Darcy velocity and  $\mathbf{U}$  is mean interstitial velocity *with respect to the solid phase*. The term  $T_z$  is due to the advection of heat in both phases by the pulling speed  $V$ , which has been scaled to unity. This elliptic equation can be solved without reference to any internal boundary conditions, as the temperature field will be continuous with continuous first and second derivatives under our present assumptions.

We employ a streamfunction-vorticity formulation, so that this equation actually takes the form

$$\nabla^2 T = -\psi_z T_x + \psi_x T_z - T_z, \quad (3.1)$$

$$(3.2)$$

where the stream function satisfies  $\mathbf{u} = (-\psi_z, \psi_x)$ . The steady solutions are approached via an artificial time-step and the ADI method, with the advective terms treated explicitly.

In terms of the total fluid velocity  $\mathbf{q}$ , the solute equation within liquid regions takes the simple form

$$\mathbf{q} \cdot \nabla C = 0,$$

implying that solute is passively advected along streamlines. Thus, there is no buoyancy within liquid regions whose streamlines emerge from the uniform source of solute which we pose as an inlet condition at the top of the computational domain. Streamlines coming from the mushy zone retain the value of the concentration they emerge with. Numerically, this is accomplished by vertically interpolating the values of  $C$  and  $\psi$  on the portion of the mush-liquid boundary with flow from mush to liquid and fitting this data via a cubic least-squares approximation to arrive at a function  $C(\psi)$  which can be employed in the buoyancy term within the plume. Finally, within the mushy zone, an equilibrium constraint is enforced so that the concentration is slaved to the temperature field via the liquidus curve in the phase diagram. The situation is further simplified by scaling and the assumption of a linear liquidus so that the interstitial concentration satisfies

$$C = T.$$

The liquidus constraint requires the solid fraction to adjust so that the bulk composition,

$$\xi = (1 - \phi)T + \mathcal{C}\phi, \tag{3.3}$$

is conserved:

$$\xi_z = \mathbf{u} \cdot \nabla C. \tag{3.4}$$

The material parameter  $\mathcal{C}$  can be thought of the nondimensional concentration in the solid phase, though the dimensional concentration is one in a model with complete solute rejection, which is what we have here.

This equation is treated by simple numerical quadrature and explicit discretization of the advective term. The solid fraction is then evaluated via (3.3). Note that this is a hyperbolic equation for the solid fraction; a fact that remains even if one restores the elliptic character of (3.4) for the concentration by considering the effects of solutal diffusivity. Thus, it is essential that the integration begin at the solidification front and follow the vertical characteristics for the solid fraction; if there are dissolved regions of the mushy zone, this integration must stop if a solute balance across a would-be dissolving interface indicates there is not enough

solute available or if the solid fraction is reduced to zero. We discuss this further below, when we address interfacial conditions.

Following our earlier work, we model flow within the mushy zone as Darcy flow with a solid-fraction-dependent permeability,

$$\Pi = (1 - \phi)^3,$$

which is one choice among many possible permeability–porosity relationships. Taking the curl of Darcy’s equation to eliminate the pressure gradient gives

$$\nabla^2 \psi = -Ra \Pi T_x + (\nabla \Pi \cdot \nabla \psi) / \Pi, \quad (3.5)$$

where  $Ra$  is a solutal-porous-medium Rayleigh number.

Within the liquid region, we assume Stokes flow, which corresponds to infinite Prandtl number. This assumption is readily relaxed, but at the cost of an additional parameter and the potential for introducing instabilities within the plume. In terms of stream function and vorticity  $\omega = \nabla \times \mathbf{u}$  we have

$$\nabla^2 \omega = -\frac{Ra}{Da} C_\psi \psi_x, \quad (3.6a)$$

$$\nabla^2 \psi = -\omega, \quad (3.6b)$$

where the buoyancy term, which is amplified by the (small) Darcy number  $Da$ , is either zero or evaluated via the interpolating function  $C(\psi)$  described above. Like the heat equation, the elliptic operators in the previous three equations are supplemented with an artificial time-step and relaxed to steady state via the ADI method with explicitly treated nonlinear terms.

We proceed iteratively from the thermal field, to the flow field, then update the solid-fraction, permeability and solute-interpolation function. For simplicity, the stream-function in the entire domain is updated via both sets of operators and then combined on the basis of phase to form the actual stream function. This is where the assumptions regarding continuity of velocity and vorticity come into play.

Turning our attention to the boundary conditions, on the exterior of the computational domain, we have

$$\psi_z = \omega_z = C = 0, T = T_0 \quad \text{at } z = H, \quad (3.7a)$$

$$\psi = 0, T = -1 \quad \text{at } z = 0, \quad (3.7b)$$

$$\psi = T_x = 0 \quad \text{at } x = 0, L, \quad z < h(x), \quad (3.7c)$$

$$\psi = \psi_{xx} = T_x = C_x = 0 \quad \text{at } x = 0, L, \quad z > h(x), \quad (3.7d)$$



where  $L$  and  $H$  are the (scaled) horizontal and vertical dimensions of the computational domain and  $h(x)$  is the position of the mush–liquid interface. Assumptions we have made concerning continuity of velocity and temperature reduce the need for internal boundary conditions; those that remain concern the interface position, which, as explained above, is needed to correctly determine the solid fraction.

As explained in Schulze & Worster (1999), the conditions which determine solid fraction and concentration at the interface along with the interface condition in the model we have presented vary depending upon both the direction of flow and the front velocity. Along most of the mush–liquid interface, flow will be into the mushy zone along a freezing interface, having arrived from the far-field carrying a uniform concentration of solute. This fact, combined with the liquidus constraint tells us that the  $T = 0$  isotherm marks the point where mush begins to form along this type of boundary. Conservation of solute can be used to show that the solid fraction there is zero. The solid fraction below the interface is then determined by integrating (3.4) downward toward the eutectic front. Vertical interpolation of the temperature field is used to evaluate the solid fraction at the first grid point in the mush. This integration should be terminated before reaching the eutectic front if the solid fraction drops below a critical value dictated by conservation of solute:

$$\phi = \frac{[C]_l^m \hat{\mathbf{n}} \cdot \mathbf{q}}{(\theta - \mathcal{C})}. \quad (3.8)$$

This critical value is zero whenever the flow is from the mush into the liquid, since the concentration must be continuous in that case, the fluid lacking any means to produce a discontinuity. If this happens, the region below this portion of the interface is once again liquid, but the streamlines will now be rising to meet this dissolving interface, having emerged from the mushy layer at a some point below. The point at which one should resume computing the solid fraction is then given by (2.1). Vertical interpolation is again used to determine the solid fraction at the first point below the interface.

## 4. Discussion of Numerical Results

The immediate results of the current paper are two-fold and are primarily aimed at testing the utility of the the boundary condition  $\mathbf{q} \cdot \hat{\mathbf{n}} = 0$ . Firstly, we discuss the solution presented in Figure 2, which represents a fully developed chimney that is a steady, stable solution of the model we described in Section 2. This is an important step forward because chimneys have never been computed using the free-boundary formulation and without exhibiting such solutions it is difficult to be sure the model is valid. For example, one could question whether the gross features of the chimney morphology, like its aspect ratio, would come out

correctly or whether it might be necessary to build some anisotropy into the permeability function in order to account for the internal morphology of the mushy layer. As explained above, the current computations take some license with the interfacial condition for the pressure/vorticity, but the qualitative features of the solution in Figure 2 are reassuring.

A secondary point of interest is the existence of the solutions that consist of liquid inclusions. These are of some interest because they illustrate all four types of boundary conditions for ideal mushy layers and may lend some insight into the mechanisms by which chimneys form in time-evolving mushy layers. It appears, however, that these solutions exist for an extremely narrow range of parameter values. They are very difficult to resolve and the boundary conditions along the top of the inclusion are difficult to implement. The solution presented in Figure 1 actually uses the condition  $\phi = 0$  along the entire top of the inclusion. We have computed solutions using the full set of boundary conditions, but it is necessary to adjust the parameters so that the inclusion takes up a larger portion of the domain, making it possible to accurately determine the normal to this interface. The solution presented here has the merit of sharing most of the same parameter values as that shown in Figure 2. The difference between this and a solution obtained using (3.8) is minute.

## Acknowledgements

This work was funded by the Engineering and Physical Sciences Research Council (UK) and by the University of Tennessee through a Professional Development Award. The authors are grateful for this support.

## References

- Amberg, G. & Homsy, G.M. 1993 Nonlinear analysis of buoyant convection in binary solidification with application to channel formation. *J. Fluid Mech.* **252**, 79–98.
- Beckermann, C. & Wang, C.Y. 1995 Multiphase/scale modeling of alloy solidification. *Ann. Rev. Heat Trans.* **6**, 115–198.
- Roberts, P.H. & Loper, D.E. 1983 Towards a theory of the structure and evolution of a dendrite layer. *Stellar and Planetary Magnetism*, ed. A.M. Soward, 329–349.
- Schulze, T.P. & Worster, M. G. 1998 A numerical investigation of steady convection in mushy layers during the directional solidification of binary alloys. *J. Fluid Mech.* **356**, 199–220.

Schulze, T.P. & Worster, M. G. 1999 Weak convection, liquid inclusions and the formation of chimneys in mushy layers. *J. Fluid Mech.* **388**, 197–215.

Worster, M.G. 1997 Convection in mushy layers. *Ann. Rev. Fluid Mech.* **29**, 91-122.

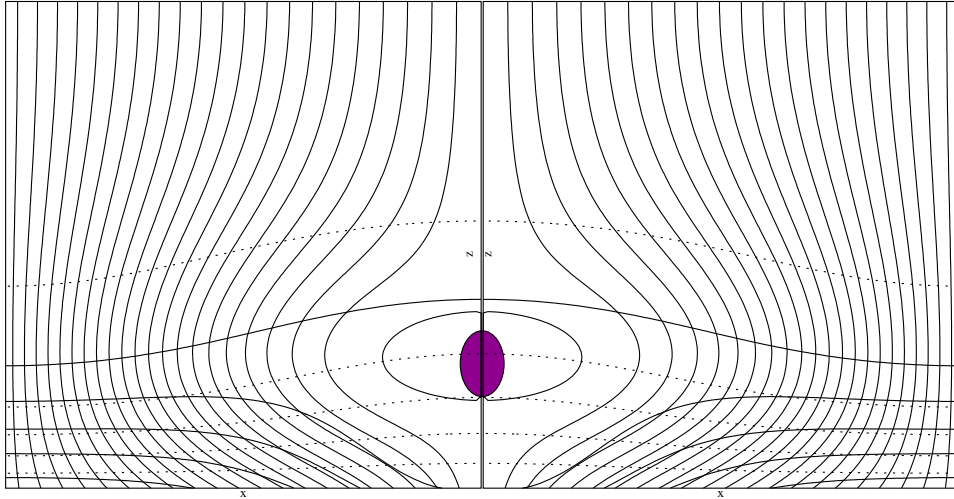


Figure 1: A steady solution with a liquid inclusion. In this figure both solid-fraction contours and streamlines are represented by solid curves and a isotherms are shown with dashed curves. In particular, the zero-solid-fraction contours include both the  $T = 0$  isotherm and the boundary of the liquid inclusion, which is shaded.

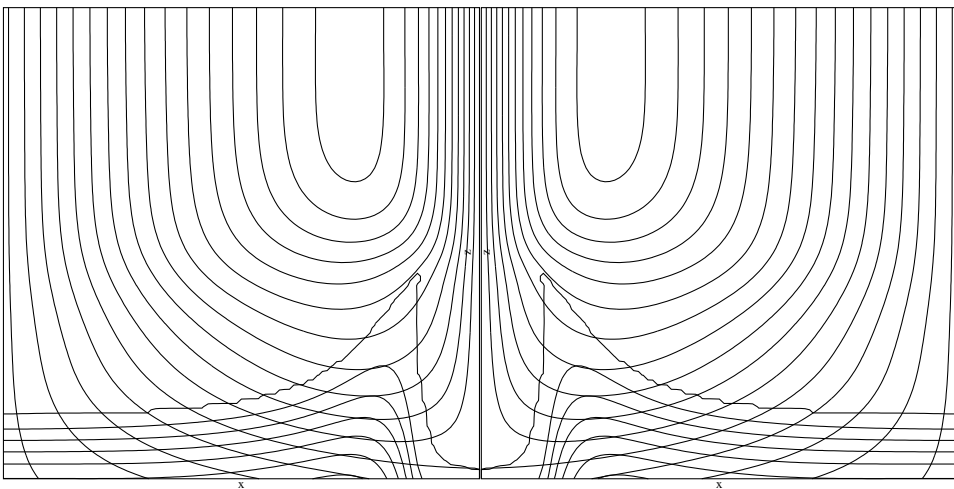


Figure 2: A steady solution with a chimney.